Appl. Phys. A 87, 171–174 (2007)
DOI: 10.1007/s00339-006-3837-0

Applied Physics A
Materials Science & Processing

Y. LIU[1]
N. FANG[2]
D. WU[1]
C. SUN[1]
X. ZHANG[1,✉]

Symmetric and antisymmetric modes of electromagnetic resonators

[1] NSF Nanoscale Science and Engineering Center (NSEC), 5130 Etcheverry Hall, University of California, Berkeley, CA 94720-1740, USA
[2] University of Illinois, Urbana-Champaign, Dept. of Mechanical & Industrial Engineering MC-244, 158 Mechanical Engineering Bldg. 1206 W. Green St., Urbana, IL 61801, USA

Received: 31 August 2006/Accepted: 15 November 2006
Published online: 24 January 2007 • © Springer-Verlag 2007

ABSTRACT In this paper, we numerically study a new type of infrared resonator structure, whose unit cell consists of paired split-ring resonators (SRRs). At different resonant frequencies, the magnetic dipoles induced from the two SRRs within one unit cell can be parallel or antiparallel, which are defined as symmetric and antisymmetic modes, respectively. Detailed simulation indicates that the symmetric mode is due to magnetic coupling to resonators, in which the effective permeability could be negative. However, the antisymmetric mode originating from strong electric coupling may contribute to negative effective permittivity. Our new electromagnetic resonators with pronounced magnetic as well as electric responses could provide a new pathway to design negative index materials (NIMs) in the optical region.

PACS 78.20.Ci; 73.20.Mf; 42.25.Bs

1 Introduction

In 1968, Veselago theoretically proposed negative index materials (NIMs) that have simultaneous negative permittivity (ε) and negative permeability (μ) [1]. It is found that many fundamental electromagnetic phenomena, such as Snell's law, Cerenkov radiation and Doppler effect reverse when NIMs are involved. However, natural materials do not possess negative refractive index, which impeded the research progress on NIMs. Only until the early twenty-first century, using metallic wires and split ring resonators (SRRs) to engineer effective permittivity (ε_{eff}) and effective permeability (μ_{eff}) respectively, have people been able to implement artificial NIMs and experimentally demonstrate the reversed Snell's law (i.e., negative refraction) [2]. Ever since then, explosive research interest in NIMs has been rekindled, and rapid progress in this area has been achieved. For instance, SRRs, as the key building block for NIMs, have demonstrated negative permeability from microwave up to telecommunication frequencies as SSRs are scaled down from millimeter to nanometer size [3–5]. In addition to the fundamental research significance, NIMs also have great application potentials. One example is the so-called superlens, which can beat the diffraction limit in conventional optics by enhancing evanescent fields to establish sub-wavelength imaging resolution [6, 7].

So far, SRRs are the most common element to realize negative permeability for constructing NIMs. From the viewpoint of equivalent circuit, an SRR can be considered as a RLC circuit with the natural resonant frequency given by $\omega_0 = \sqrt{1/LC}$, where L and C are the geometric inductance and capacitance of the SRR structure, respectively [8]. Within a certain frequency region centered at ω_0, the magnetic flux threading through SRRs induces a strong circulating current, resulting in an effective magnetic dipole. This induced magnetic dipole can respond in phase (i.e., $\mu_{\text{eff}} > 1$) or out of phase (i.e., $\mu_{\text{eff}} < 1$) with respect to the external field. If the strength of magnetic response is sufficiently strong, negative μ_{eff} can be achieved. Very recently, simplified magnetic resonators have demonstrated negative μ_{eff} in the telecommunication and visible region [9, 10], although the working principle still relies on the RLC resonance.

Inspired by the work of Nordlander et al. on the electric-dipole interaction of two metallic nanoparticles [11], in this paper we investigate a new type of electromagnetic resonators working at infrared frequencies, whose unit cell consists of paired ring resonators (PRRs). It is found that the induced magnetic dipoles from the two ring-resonators within one unit cell can be parallel or antiparallel, which are termed as symmetric and antisymmetic modes in the paper, respectively. Detailed simulations indicate that the two modes have different physical mechanisms. The symmetric mode originates from the magnetic coupling to the resonator, in which the effective permeability could be negative. However, the antisymmetric mode is due to strong electric coupling, which may contribute to negative effective permittivity. In other words, PRRs possess both pronounced magnetic and electric responses. This result provides deeper insights into traditional SRRs. More importantly, it suggests that ring-type resonators could replace wire media to produce negative ε_{eff}. Therefore, we expect that NIMs may be created by combing two sets of electromagnetic resonators.

2 Simulation and discussion

Figure 1a illustrates the geometry of the paired-ring resonators (PRRs), which comprise two horizontal C-shaped SRRs in one unit cell. The lattice constant $a = 600$ nm,

✉ Fax: +1-510-643-2311, E-mail: xiang@berkeley.edu

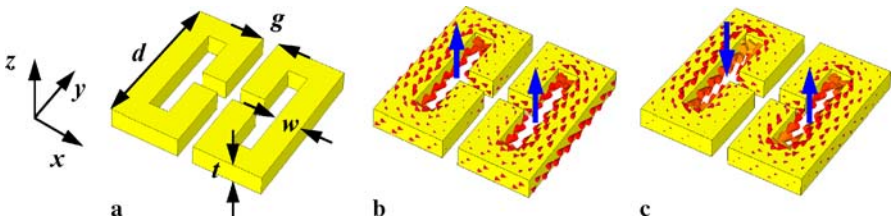

FIGURE 1 (**a**) The schematic of a paired-ring resonator (PRR), where the element dimension $d = 500$ nm, line width $w = 80$ nm, gap $g = 50$ nm, metal (*gold*) thickness $t = 50$ nm and lattice constant $a = 600$ nm. (**b**) and (**c**) show the surface currents of the first two eigenmodes of the PRR structure, which resonate at 90.5 THz and 130.4 THz, respectively. In (**b**), surface currents induce two parallel magnetic dipoles as indicated by the blue *arrows*. This mode is defined as the symmetric mode of PRRs, while in (**c**) surface currents induce two anti-parallel magnetic dipoles, corresponding to the antisymmetric mode of PRRs

element dimension $d = 500$ nm, line width $w = 80$ nm, gap $g = 50$ nm and metal (gold) thickness $t = 50$ nm. Using Microwave Studio by CST, a commercial electromagnetic solver based on the finite difference time domain (FDTD) algorithm, we first simulate the eigenmode of the resonator. Figure 1b and c show the surface current density for the first two eigenmodes at 90.5 THz and 130.4 THz, respectively. From the circulation direction of surface currents, it is straightforward to find that the induced magnetic dipole moments of the two SRRs are parallel for the first eigenmode, while antiparallel for the second one. We term the two cases as symmetric and antisymmetric mode, respectively. In [11], the dimer-plasmon resonance is studied. Due to the interaction of two electric dipoles, the bonding (symmetric) and antibonding (antisymmetric) mode can be formed for a dual-particle system. The arising question is whether the symmetric and antisymmetric modes of PRRs are attributed to magnetic-dipole interaction.

To reveal the physical origin of the symmetric and antisymmetric mode, *S*-parameter for a single unit is calculated with open boundary conditions along the wave propagation,

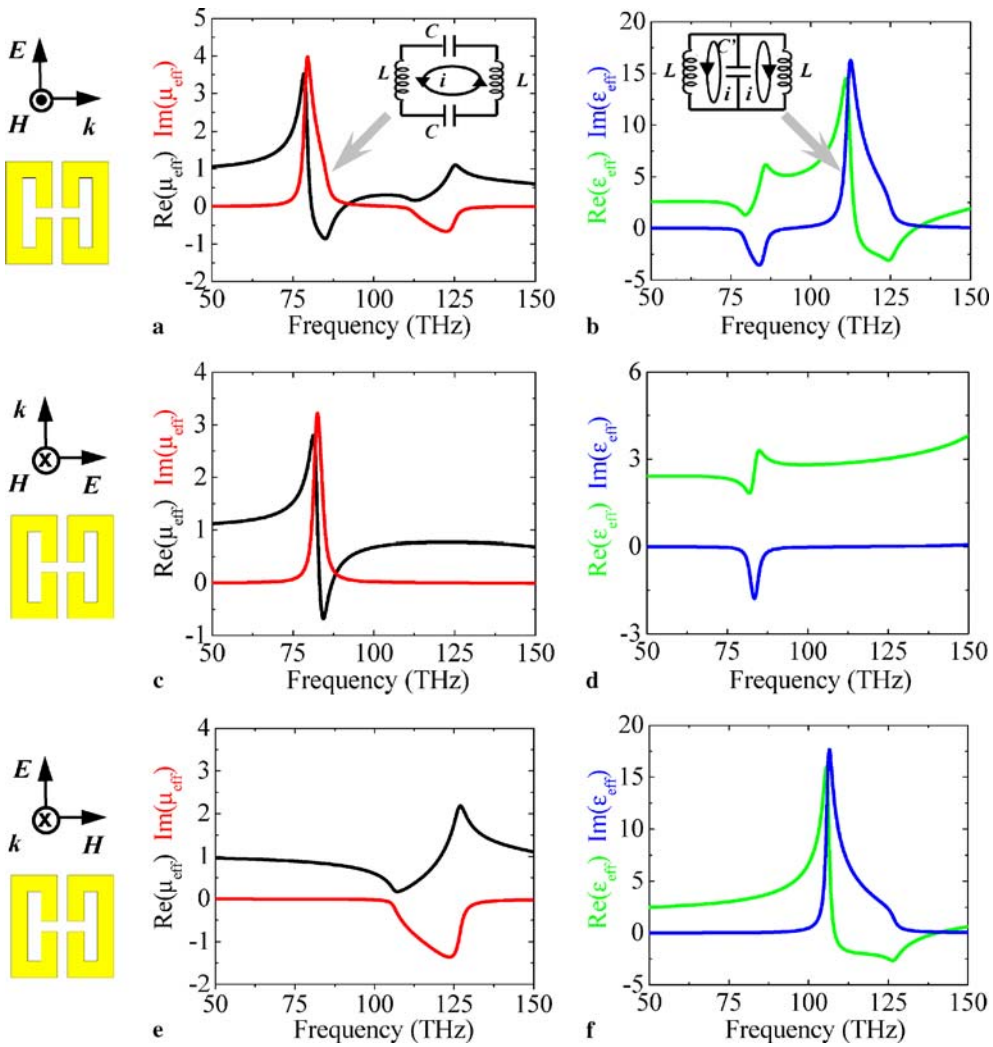

FIGURE 2 Effective material properties of PRRs under different excitation conditions. In (**a**) and (**b**), both magnetic and electric fields can couple to PRRs and induce resonances. The first resonance around 83 THz of PRRs originates from the magnetic coupling, which is indicated by the Drude–Lorentz resonance behavior in the μ_{eff} curve around 83 THz (see (**a**)). Accompanying this magnetic resonance, there is an anti-Drude–Lorentz resonance in the ε_{eff} curve (see (**b**)). The second resonance centered at 115 THz is due to the electric coupling. Around 115 THz, there is a strong Drude–Lorentz resonance behavior in the ε_{eff} curve (see (**b**)), while an anti-Drude–Lorentz resonance co-exists in the μ_{eff} curve (see (**a**)). The *inset* of (**a**) and (**b**) illustrates the equivalent circuit for the magnetic resonance and electric resonance, respectively. From the equivalent circuits, it can be seen that the magnetic resonance induce currents circulating along the whole structure in phase, giving rise to the symmetric mode of PRRs. On the contrary, the electric field coupled to the resonator induces two anti-parallel magnetic dipoles, corresponding to the antisymmetric mode of PRRs. Under the excitation condition for (**c**) and (**d**), only magnetic resonance exists around 83 THz. Under the excitation condition for (**e**) and (**f**), there is only an electric resonance centered at 115 THz

and electric and magnetic boundary conditions on the transverse direction. Then effective material properties (i.e., ε_{eff} and μ_{eff}) can be extracted from the *S*-parameter [12]. Figure 2 plots the dispersion curves of ε_{eff} and μ_{eff}. It can be seen that around 83 THz, μ_{eff} has a strong Drude–Lorentz resonance behavior with the real part raging from 3.5 to –1. This indicates that the first resonance results from a magnetic response of PRRs. Interestingly, there is an anti-Drude–Lorentz resonance in the ε_{eff} curve around 83 THz, although ε_{eff} never reaches negative values. This electric anti-resonance is caused by the bounded refractive index of the structure which possesses intrinsic finite periodicity [13]. At around 112 THz, ε_{eff} has a clear Drude–Lorentz resonance with ε_{eff} dramatically changing from 15 to –3.5. Accordingly, effective permeability has an anti-resonance behavior.

The inset of Fig. 2a and b illustrates the equivalent circuit for the magnetic resonance and electric resonance, respectively, enabling us to have better understanding of the different mechanisms for the two resonances. For the first magnetic resonance, the normal component of the magnetic field (H_z) penetrating a single unit cell induces currents circulating along the whole structure. The resulting magnetic moment of each sub-SRR oscillates in phase, which gives rise to the symmetric mode. Electric fields (E_y) can also couple to the resonator by capacitors (the vertical gap of each SRR), and drive currents to flow in opposite directions as illustrated the inset of Fig. 2b. This is the origin of the antisymmetric mode, which results from electric coupling.

In order to further verify the above analysis about the resonance mechanism, effective permeability and permittivity of the structure is calculated under different excitation conditions. For Fig. 2c and d, the external field propagates along the *y*-axis, and the magnetic filed is normal to the PRRs (i.e., *H* is along the *z*-axis). It is expected that the magnetic field can still excite the resonator, which is confirmed by the Drude–Lorentz resonance behavior near 83 THz in Fig. 2c. However, since the electric field is parallel to the capacitor (vertical gap) of SRRs, the electric field cannot couple to the resonator. Therefore, there is no apparent electric resonance for frequencies up to 150 THz (note the anti-resonance around 83 THz in the dispersion curve of ε_{eff} is an "antifact" due to the periodicity of the structure). For Fig. 2e and f, the wave vector $\boldsymbol{k}$ is normal to PRRs. Obviously, there is no magnetic resonance since the magnetic field is completely parallel to the PRRs plane; while the in-plane electric field can still couple to the resonator to induce a strong electric resonance, giving rise to negative ε_{eff} in a wide frequency region (from 107 THz to 138 THz). From the systematic simulation on the effective properties of PRRs under different excitation conditions, we can draw a conclusion that the magnetic field induced resonance of PRRs drives the surface current of two sub-SRRs oscillating in phase, which leads to the symmetric mode of PRRs; however, electric fields can couple to PRRs and induce currents circulating along the two sub-SRRs out of phase, which results in the anti-parallel magnetic dipoles (i.e., the antisymmetric mode of PRRs).

A different infrared PRR, whose unit cell has two SRRs sharing a middle arm with width *l* as illustrated in Fig. 3a, is also studied. Under the same excitation condition as that of Fig. 2a and b, this PRR also possesses strong magnetic and electric resonances. However, the electric resonance frequency of PRRs (about 70 THz) is lower than the magnetic resonance (about 115 THz), which can be seen in the μ_{eff} (Fig. 3b) and ε_{eff} (Fig. 3c) curve. The inset of Fig. 3b and c plot the surface current at the electric and magnetic resonance, respectively. Once again, the electric resonance induces currents circulating out of phase in the two sub-SRRs, giving rise to the antisymmetric mode as we discussed before. In contrast, the magnetic resonance can produce two parallel magnetic dipoles, which is the origin of the symmetric mode.

The width of the middle arm can strongly influence the electric resonance, while it has less effect on the magnetic one. This is because at the electric resonance, the induced currents of each sub-SRR converge to the middle arm; however there are almost no surface currents on the middle arm as the magnetic resonance takes place. Figure 4 plots the transmission

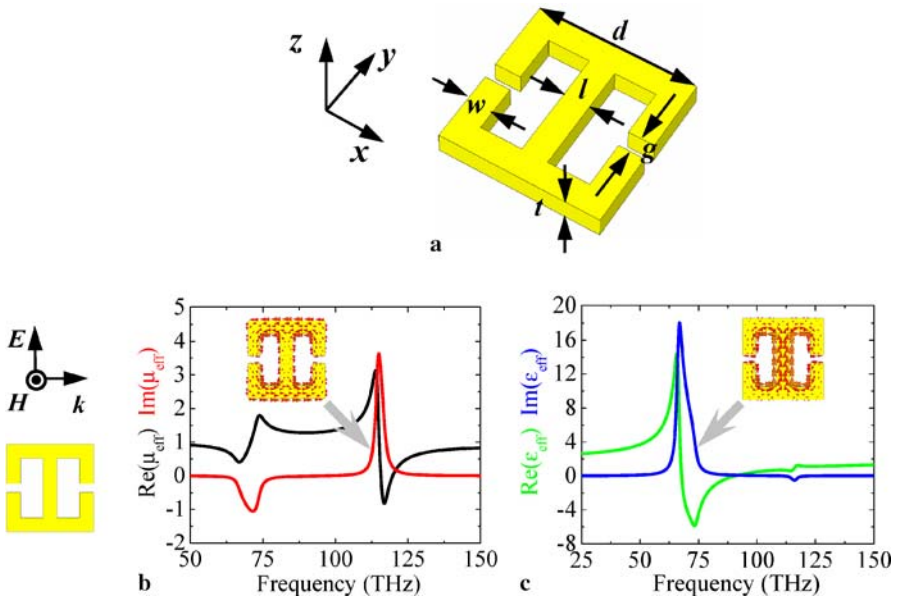

FIGURE 3 (**a**) Schematic of a different type of PRR, in which two SRRs are sharing a middle arm with width $l = 80$ nm. Other parameters are: $d = 500$ nm, $w = 80$ nm, $g = 50$ nm, $t = 50$ nm and lattice constant $a = 600$ nm. (**b**) and (**c**) are frequency-dependent μ_{eff} and ε_{eff} curves, respectively, under the same excitation condition as Fig. 2a and b. The first resonance is due to the electric coupling, while the second one is magnetic-field induced resonance. The *insets* of (**b**) and (**c**) show the surface currents for the magnetic and electric resonances, respectively, which indicate that the magnetic resonance gives rise to the symmetric mode, while the electric resonance produces the anti-symmetric mode

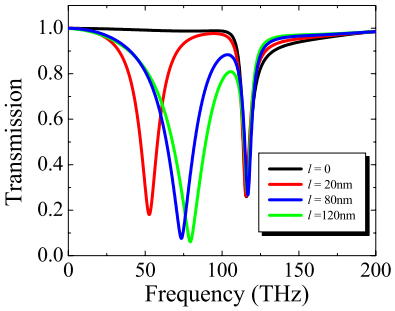

FIGURE 4 Transmission spectra of PRRs for varied width of the middle arm (see the schematic illustration in Fig. 3a) under the same excitation condition as Fig. 3. The electric resonance (in the low-frequency region) is highly dependent on l, while the magnetic resonance is insensitive to l

spectra as changing the width of the middle arm. As expected, the magnetic resonance frequency has small shifts, nevertheless the electric resonance shifts to higher frequencies when the width of the middle arm increases.

Based on the systematic simulation on two different PRRs, it can be seen that PRRs have strong electric resonance in addition to the magnetic one. Depending on the orientation of the structure with respect to the external field, effective permittivity and (or) effective permeability can achieve considerably negative value in the mid-infrared region. As pointed out by [14], electromagnetic resonators with negative ε_{eff} have potential advantages over conventional metallic wires in the future design of NIMs. Metallic wires are required to be continuous to obtain negative ε_{eff}, which is rather challenging in three-dimensional (3D) NIMs. On the contrary, electromagnetic resonators can be considered as local electric or magnetic particles. It is relatively easier to assemble those particles to construct 3D NIMs. Our PRR structure possesses both remarkable electric and magnetic resonances, which provides a flexible element for the future metamaterial design.

As discussed in the introduction, similar to two metallic particles which can form bonding (symmetric mode) and antibonding (anti-symmetric mode) due to electric-dipole (and higher-order mode) coupling, we expect that when two SRRs are placed together, two new modes will be established, completely originating from the magnetic dipole interaction. In the PRR structure we studied in this paper, symmetric modes and antisymmetric modes are observed. However, they are not resulting from direct magnetic dipole interaction, but from magnetic coupling and electric coupling of external fields to the resonator, respectively. The reason is that when two SRRs are horizontally positioned, the induced-dipoles are arranged side by side, and therefore the interaction between neighboring magnetic dipoles is not strong enough to induce the energy split. In the case that two SRRs are vertically arranged and close to each other, the magnetic bonding and antibonding effects are expected.

3 Conclusion

We have studied paired ring resonators (PRRs), whose unit cell consists of two horizontally-placed split ring resonators (SRRs). It is found that the induced magnetic dipoles from the two SRRs can orientate symmetrically or antisymmetically. Detailed simulations under different excitation conditions show that the symmetric and antisymmetric modes have different physical mechanisms, which originates from the magnetic coupling and electric coupling, respectively. Our proposed electromagnetic resonators possess both pronounced magnetic and electric responses, which provide new building blocks for the design of negative index materials in the optical region.

ACKNOWLEDGEMENTS This research was partially supported by the NSF Nanoscale Science and Engineering Center (NSEC) under award number DMI-0327077 and the DARPA Negative Index Materials (NIM) program (HR 0011-05-3-0002).

REFERENCES

1 V.G. Veselago, Sov. Phys. Uspekhi **10**, 509 (1968)
2 R.A. Shelby, D.R. Smith, S. Schultz, Science **292**, 77 (2001)
3 D.R. Smith, W.J. Padilla, D.C. Vier, S.C. Nemat-Nasser, S. Schultz, Phys. Rev. Lett. **84**, 4184 (2000)
4 T.J. Yen, W.J. Padilla, N. Fang, D.C. Vier, D.R. Smith, J.B. Pendry, D.N. Basov, X. Zhang, Science **303**, 1494 (2004)
5 C. Enkrich, M. Wegener, S. Linden, S. Burger, L. Zschiedrich, F. Schmidt, J.F. Zhou, T. Koschny, C.M. Soukoulis, Phys. Rev. Lett. **95**, 203 901 (2005)
6 J.B. Pendry, Phys. Rev. Lett. **85**, 3966 (2000)
7 N. Fang, H. Lee, C. Sun, X. Zhang, Science **308**, 5721 (2005)
8 J.B. Pendry, A.J. Holden, D.J. Robbins, W.J. Stewart, IEEE Trans. Microw. Theory Technol. **47**, 2075 (1999)
9 G. Dolling, C. Enkrich, M. Wegener, J.F. Zhou, C.M. Soukoulis, S. Linden, Opt. Lett. **30**, 3198 (2005)
10 A.N. Grigorenko, A.K. Geim, H.F. Gleeson, Y. Zhang, A.A. Firsov, I.Y. Khrushchev, J. Petrovic, Nature **438**, 335 (2005)
11 P. Nordlander, C. Oubre, E. Prodan, K. Li, M.I. Stockman, Nano Lett. **4**, 899 (2004)
12 D.R. Smith, S. Schultz, P. Markos, C.M. Soukoulis, Phys. Rev. B **65**, 195 104 (2002)
13 T. Koschny, P. Markos, E.N. Economou, D.R. Smith, D.C. Vier, C.M. Soukoulis, Phys. Rev. B **71**, 245 105 (2005)
14 D. Schurig, J.J. Mock, D.R. Smith, Appl. Phys. Lett. **88**, 041 109 (2006)